



# Microstructures and mechanical properties of 25Cr duplex stainless steel

Chatchai MEENA and Vitoon UTHAISANGSUK\*

King Mongkut's University of Technology Thonburi, 126 Pracha Uthit Road, Bang Mod, Thung Khru, Bangkok 10140, Thailand

\*Corresponding author e-mail: vitoon.uth@kmutt.ac.th

**Received date:**

5 June 2019

**Revised date:**

4 September 2019

**Accepted date:**

6 October 2019

**Keywords:**

Duplex stainless steel  
Mechanical properties  
Precipitates

**Abstract**

Recently, the demand of duplex stainless steels has been continuously increased in different types of application, especially, tubing of heat exchanger, thermal generator, vessels and pumps. The duplex steel grades exhibit high strength property and excellent corrosion resistance. However, after welding and heat treatment their toughness and corrosion resistance could be significantly decreased due to the occurrences of various detrimental intermetallic phases like sigma phase. In this work, effect of heat treatment on microstructure and mechanical behavior of super duplex stainless steel grade SAF 2507 were investigated. Firstly, samples of the examined steel were heat-treated at the temperature of 850°C for different holding times. Then, microstructure evolutions of heat-treated samples were characterized by an optical and scanning electron microscopy. The emerged phases were identified, their phase fractions were determined and the Vickers hardness tests were performed for the different phase constituents. In addition, tensile tests and Charpy impact tests of heat-treated specimens were carried out. The steel samples subjected to the holding time of 90 min exhibited significantly deteriorated toughness property. This was caused by large amount of occurred brittle intermetallic precipitates.

## 1. Introduction

Duplex stainless steels (DSSs) are widely employed in various tubing of chemical, petrochemical plants, in heat exchanger of power plant, separators, as well as deep water pipe [1,2]. These steel grades provide a great combination of advantageous mechanical properties and excellent corrosion resistance. On a micro-scale, the steels have typically multiphase microstructures consisting of austenite, ferrite and some intermetallic phases. Due to their high strength characteristic reduced wall thickness is also allowed for lightweight structural design. By some applications, duplex stainless steels need to be often jointed with other low or high alloyed tubes with regard to required installation and maintenance works. During the welding and pre- or post-heat treatment processes, ferrite, sigma phase and other detrimental intermetallic phases could take place and lead to noticeably decreased toughness value as well as corrosion resistance [1,3,4]. This most likely resulted in an unexpected failure because of brittle cracking when severe load or pressure was applied. It was shown that occurred sigma phase and precipitations in DSSs were the most crucial factors for their performance restrictions [5]. In it was reported that the sigma phase could lead to deteriorated mechanical properties of cast DSS and super DSS alloy after heat treatments and welding, respectively [6,7]. The stress-strain curve of material in the weld zone became higher than those of other areas, but the elongation was largely reduced. It is seen that the microstructure change during heat

treatment processes of DSSs is one of the important keys for the safety integrity and maintenance planning of engineering components. In this work, the DSS grade SAF 2507 was investigated. Heat treatments at the temperature of 850°C with varying holding times between 10 and 120 min were carried out for the DSS specimens. Afterwards, metallographic examinations, tensile tests and Charpy impact tests were conducted. The resulted microstructures, local hardness values, tensile properties and impact toughness of investigated specimens were correlated and discussed.

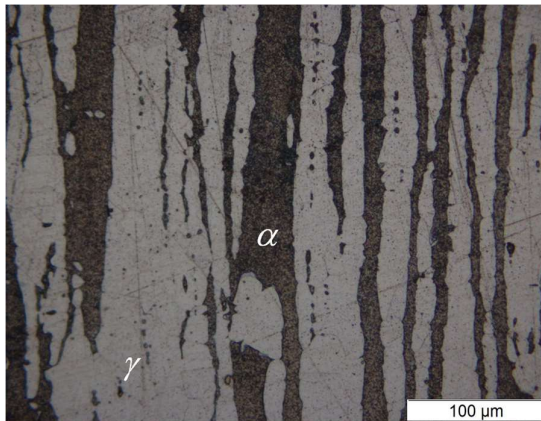
## 2. Experimental

The examined DSS grade SAF 2507 was a bulk cylinder with the initial diameter of 50 mm. Its chemical composition obtained by spectrometry analysis is shown in Table 1. The as-received DDS was firstly characterized by optical microscope (OM) and electron scanning microscope (SEM). The chemical etching was done by using a solution of 122 ml HCl, 6 ml HNO<sub>3</sub> and 122 ml H<sub>2</sub>O according to that used in N. Llorca-Isern et al [8]. As presented in Figure 1, the DSS sample consisted of austenitic ( $\gamma$ ) and ferritic ( $\alpha$ ) phase with the ratio of phase fraction of around 1:1. The gray zones are austenite and black zones are ferrite. The DSS exhibited good mechanical properties and corrosion resistance in consequence of containing phases, relatively high Mn, Mo and Cr contents. Moreover, the elongated grains were noticeably observed in the direction parallel to the extrusion direction.

**Table 1.** Chemical compositions of the examined DSS grade 2507 (in wt%).

Steel grade	C	Cr	Ni	Mn	Si	Mo	P
SAF 2507	0.03	25.03	6.20	0.82	0.50	3.52	0.03

Due to the large amount of Cr, Ni and Mo sigma phase and high Cr-precipitates can easily take place in the examined DSS samples. Such undesired precipitates would lead to various corrosions and load carrying capacity problems for example micro-galvanic corrosion [9,10]. Basically, the micro-galvanic corrosion took place between sigma phases and ferrite which led to Cr-depleted zone. This micro-galvanic process subsequently caused a micro-pitting.

**Figure 1.** Microstructure of as received DSS grade SAF 2507.

By the experiments, DSS specimens were heated up to the temperature of 850°C, held for 10, 15, 20, 30, 60 and 90 min and cooled down in still water. This temperature was selected to be approximately within the region of sigma phase precipitation. Note that this temperature range was estimated with regard to the time-temperature-transformation (TTT) diagram of similar DSS grade as shown in [3,11], which was developed on the basis of quantitative metallography results from OM and SEM. It was reported that the sigma-phase transformation in the cast alloy was somewhat slower than in the wrought alloy of the same grade. This was primarily because of their different initial microstructures. After that, metallographic analyses of all heat-treated samples were performed by both OM and SEM. Subsequently, the local chemical compositions of observed individual phases in the microstructures of as-received and heat-treated samples were determined by EDX analyses. Vickers hardness measurement was performed for each existing phases.

In addition, tensile specimens according to the EN10002 standard were prepared for the as-received DSS and DSS subjected to heat treatments with the holding times of 15 and 90 min. The tensile tests were

conducted at room temperature on a 50 kN universal testing machine and engineering stress-strain curves of tested specimens were then determined. The Charpy impact tests of DSS samples taken from the same conditions as above were carried out at room temperature. The absorbed energies of all specimens were gathered and compared.

### 3. Results and discussion

#### 3.1 Metallography analysis

From the results of metallographic examinations, it was found that the specimens heat-treated at the temperature of 850°C with varied holding times exhibited different amount and morphology of phase constituents. Figure 2(a) and 2(b) depict the SEM micrographs of samples held at 850°C for 30 and 60 mins, respectively. By holding in the two-phase ( $\alpha/\gamma$ ) region for sufficient time, the ferritic phase transformed to secondary austenite and sigma phase due to the diffusion of alloying elements from the matrix to interphases between ferrite and austenite and lower solubility of ferrite, was clearly recognized similar to the results in [12,13]. It is noted that this area would undergo a regular austenite-ferrite transformation during a continuous cooling when insufficient holding time was applied. In Figure 2, the lighter gray and smooth areas are the primary austenite, while the darker gray zones with deeper rough surface are the secondary austenite and the sigma phase was the smooth plateau among the discontinuous secondary austenite areas. The ferrite was surrounded by the occurred precipitates. With the longest holding time, no ferrite was detected as it was completely transformed to the secondary austenite and sigma phase.

This result fairly agreed with that shown in [6,13]. The local chemical compositions of individual observed phases including ferrite, austenite and precipitates in the microstructure of as-received sample and sample heat-treated at the temperature of 850°C for 90 min were determined by EDX analyses and are then provided in Table 2 and 3, respectively. Note that no precipitate was noticed in the as-received sample. The local chemical compositions of the ferritic and austenitic zone of this sample were considerably different. On the other hand, it can be seen that for the heat-treated sample the amounts of Cr and Mo in austenite and secondary austenite were greatly lower than those of the sigma phase. The regions of emerged precipitate were enriched with Cr, Ni and Mo elements similar to the results found in [11].

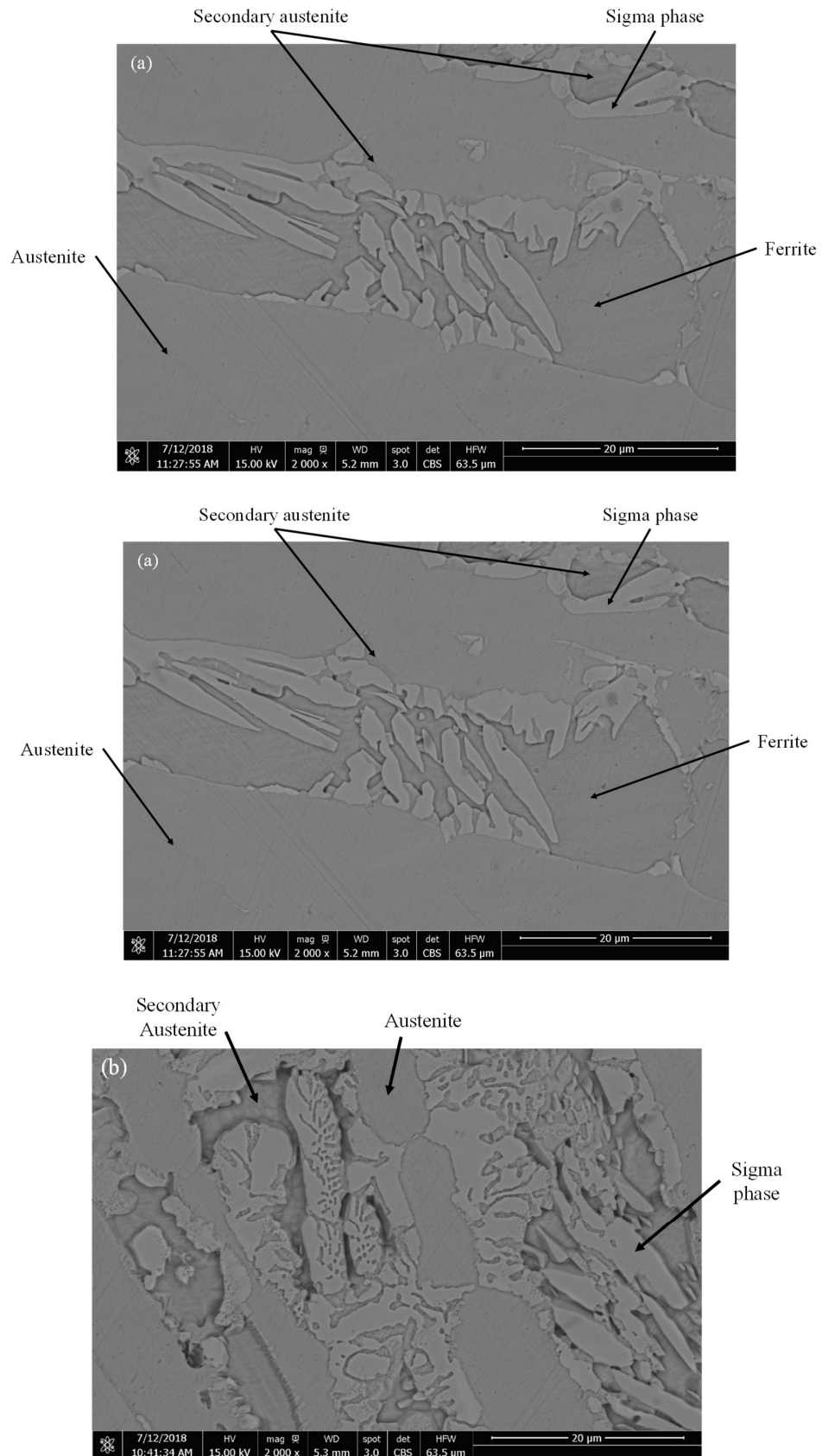


**Figure 2.** Microstructure of DSS sample heat-treated at 850°C and held for (a) 30 min and (b) 60 min.

The Cr and Mo elements, which highly accumulated in the sigma phase regions, could result in a largely increased overall hardness of DSS specimen as reported in [14]. Therefore, it might be prone to premature failure of DSS sample under loading due to brittle cracking. It was obvious that longer holding times at the temperature of 850°C led to increased amounts of the precipitates, as illustrated by microstructure observations in Figure 3. The area fractions of precipitate phases were determined by an image analysis program on the basis of color contrast of observed micrographs, as demonstrated in Figure 3 (middle row). The first row depicts the micrographs obtained by using etching method described above. Additionally, an electro-chemical etching in a solution of 10 g KOH and 100 ml H<sub>2</sub>O, which was similar to that employed in [15], was also employed and the results of corresponding microstructures are presented in Figure 3 (right row). The DSS samples heat-treated at the temperature of 850°C for 10, 15, 30, 60 and 90 min exhibited the amount of precipitates of about 1, 4, 11, 16 and 24%, respectively. The area fractions measured with regard to both etching procedures exhibited just a slight deviation of less than 10%. It is noticed that the relationship between the amount of occurred precipitates and holding time was not in a linear manner.

### 3.2 Tensile and Charpy impact test

The engineering stress-strain curves of all tested samples of examined DSS were determined and are compared in Figure 4. It is seen that the samples held at the temperature of 850°C for 90 mins showed highly reduced elongation, while the elongation of samples held for 15 mins was somewhat lower than that of as-received samples. Otherwise, the yield stresses of heat-treated samples were increased up to around 150 MPa. This pronounced brittleness of heat-treated DSS samples was caused by the occurrence of sigma phase. The resulting tensile properties were comparable with those reported in [16-18]. From the Charpy impact tests, the determined average absorbed energies of as-received specimens and specimens heat-treated at

850°C for 15 and 90 mins were 277, 40 and 5.3 J, respectively. The as-received DSS samples exhibited a highly ductile fracture behavior. Nevertheless, it is clearly seen that the DSS samples heat-treated for 90 mins showed significantly decreased impact toughness which was in accordance with the tensile test results. On the other hand, the samples heat-treated for considerably shorter holding time at 850°C just showed slightly lowered elongation, but its impact toughness was noticeably deteriorate. The influence on impact toughness in this work was similar to that found in [19]. Due to the presence of small amounts of high Cr-precipitates the toughness of DSS could be obviously decreased. Indeed, the yield and tensile strength were less affected. The effect of sigma phase on strength and toughness of DSS should be carefully and separately taken into account.

### 3.3 Micro-hardness test

The Vickers micro-hardness tests were carried out for the observed phases in DSS samples subjected to the heat treatments. The indent force of 10 kg and holding time of 5 s were applied during the measurements. Figure 5 illustrates the micro-hardness values of austenite, ferrite and precipitate in the samples heat-treated for 30 mins. It was found that the Vickers hardness values of austenitic area were about 435-450 HV and were similar in all specimens. No significant difference between hardness of ferrite and austenite was found. It is noted that the hardness of ferrite in specimens heat-treated longer than 20 mins could not be measured, because most ferrite transformed to secondary austenite and sigma phase and its areas were covered by the sigma phase. Indeed, the hardness values of precipitates in the samples with different holding times were somewhat varied and ranged from 670 to 720 HV. The hardness of precipitate phase in examined DSS samples was considerably higher than those of austenite and ferrite that was in accordance with [20]. This hard phase certainly contributed to the largely reduced impact toughness of DSS sample.

**Table 2.** Chemical compositions of each phases in as-delivered DSS grade 2507 obtained by EDX analysis (in wt%).

Regions	C	Si	Cr	Ni	Mo
$\alpha$ phase	2.73	0.61	26.70	4.04	4.45
$\gamma$ phase	2.86	0.47	23.10	7.63	2.63

**Table 3.** Chemical compositions of each phases in DSS samples heat-treated at 850°C for 90 min obtained by EDX analysis (in wt%).

Regions	C	Si	Cr	Ni	Mo
Precipitate phase	8.58	0.56	28.30	3.57	6.67
Secondary $\gamma$ phase	7.33	0.50	22.80	2.53	1.56
$\gamma$ phase	7.44	0.42	22.00	7.04	2.13

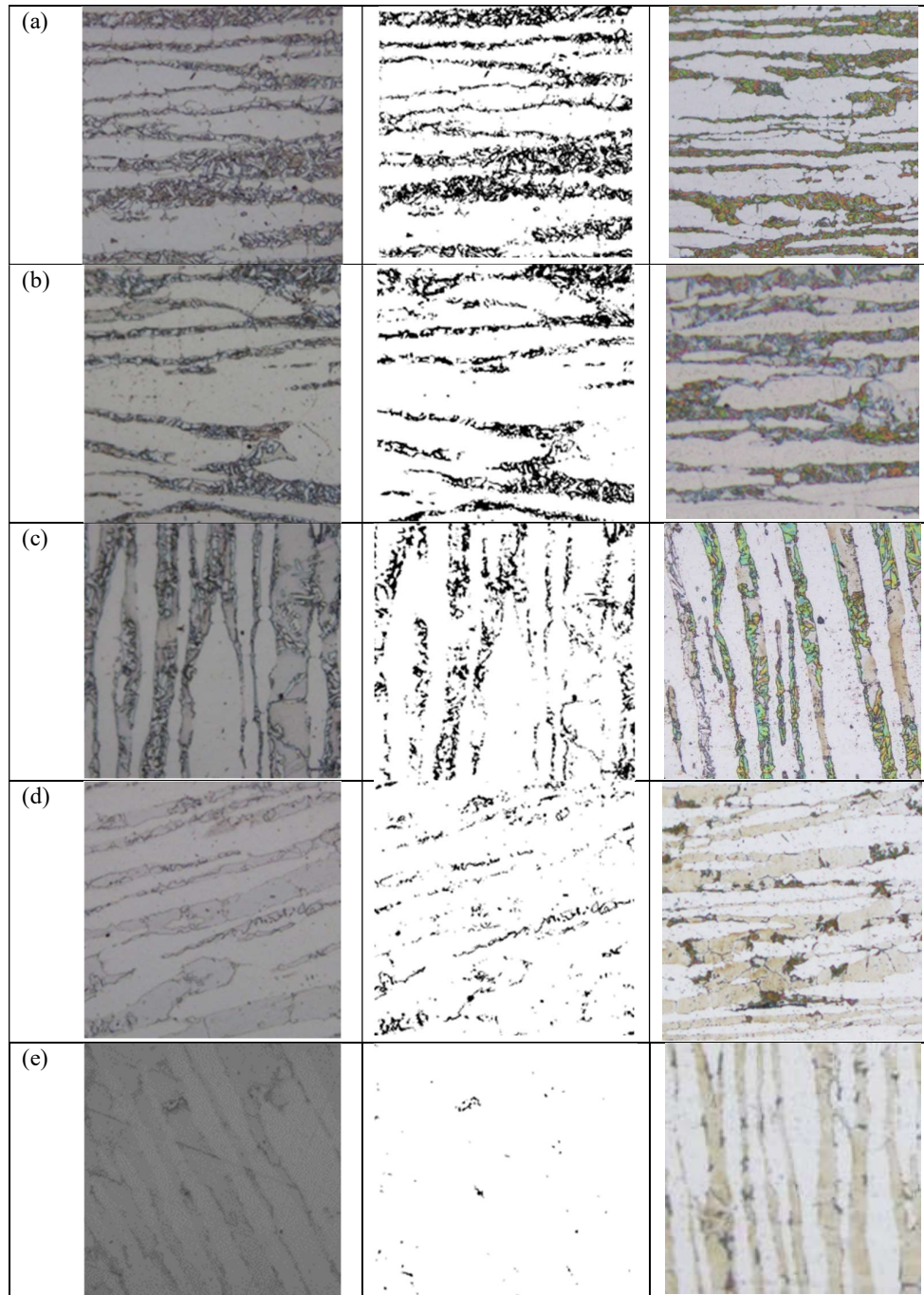


**Figure 3** Microstructures and phase characterizations of DSS specimens heat-treated at the temperature of 850°C and held for (a) 90, (b) 60, (c) 30, (d) 15 and (e) 10 min.

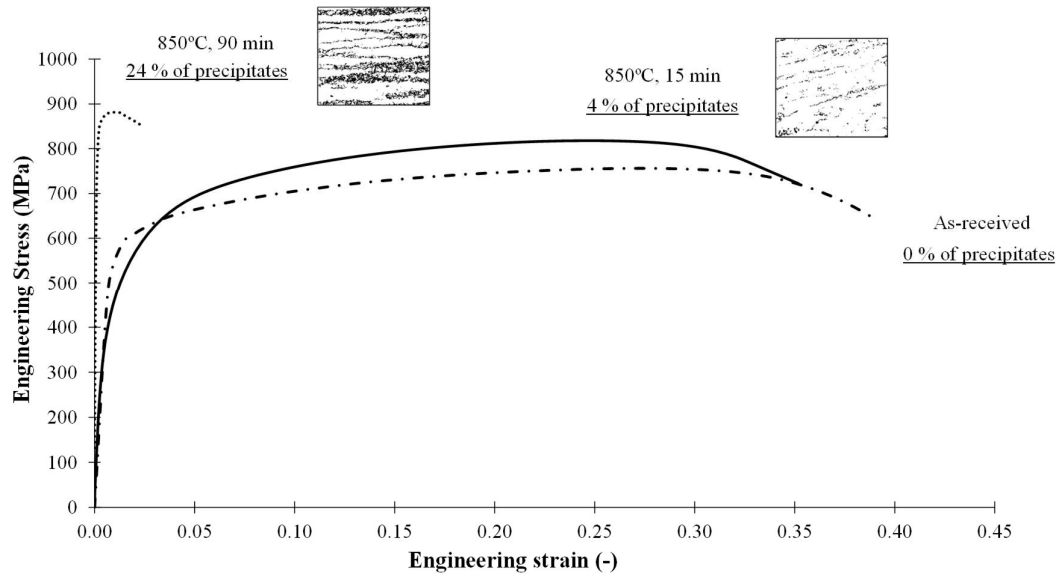


**Figure 4** Engineering stress-strain curves determined by tensile tests of samples with and without heat treatments.

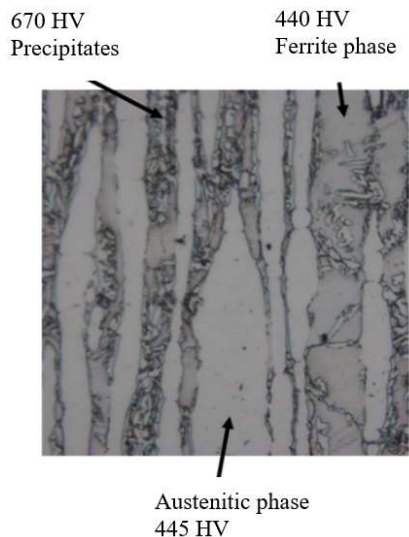


**Figure 5.** Vickers hardness values of local phases in heat-treated DSS sample.

#### 4. Conclusions

The DSS grade SAF 2507 subjected to heat treatment at the temperature of 850°C for different holding times were investigated. The amount of occurred precipitate phase, which was enriched with Cr and Mo, was increased non-linearly with the holding time. With a sufficient long holding time, significantly higher yield and tensile strength, but lowered elongation of DSS samples could be observed. Furthermore, specimens with the holding time of 90 mins, which even had about 24% precipitate area fraction, showed greatly decreased impact toughness. This considerable brittleness was due to the high hardness of emerged precipitate.

#### References

- [1] G. C. Chail and P. Kangas, "Super and hyper duplex stainless steels: structures, properties and applications," *Procedia Structural Integrity*, vol. 2, pp. 1755-1762, 2016.
- [2] I. Weibull, "Duplex stainless steels and their application, particularly in centrifugal separators. Part A History & Development," *Materials and Design*, vol. 8 (1), pp. 35-40, 1987.
- [3] C. C. Hsieh and W. Wu, "Overview of intermetallic sigma ( $\sigma$ ) phase precipitation in stainless steels," *ISRN Metallurgy*, vol. 2012, article ID 732471, 2012.
- [4] F. Tehovnik, B. Arzenek, B. Arh, D. Skobir, B. Pirnar, and B. Zuzek, "Microstructure evolution in SAF 2507 super duplex stainless steel," *Materials and Technology*, vol. 45, pp. 339-345, 2011.
- [5] J. O. Nilsson, "Super duplex stainless steels," *Materials Science and Technology*, vol. 8, pp. 685-700, 1992.
- [6] Z. H. Zhu, W. D. Zhang, X. H. Tu, X. J. Wang, and W. Li, "Effect of sigma phase precipitation on microstructure and properties of cast ZG<sub>0</sub>Cr<sub>26</sub>Ni<sub>5</sub>Mo<sub>3</sub>Cu<sub>3</sub> duplex stainless steel under different heat treatments," *China Foundry*, vol. 15 (3), pp. 182-188, 2018.
- [7] V. A. Hosseini, L. Karlsson, S. Wessman, and N. Fuertes, "Effect of sigma phase morphology on the degradation of properties in a super duplex stainless steel," *Materials (Basel)*, vol. 11 (6), pp. 933, 2018.
- [8] N. Llorca-Isern, H. Lopez-Luque, and I. Lopez-Jiménez, M.V. Biezma, "Identification of sigma and chi phases in duplex stainless steels," *Materials Characterization*, vol. 112, pp. 20-29, 2016.

- [9] J. Ding, E. H. Han, Z. Zhang, S. Wang, and J. Wang, "Influence of sigma phase on corrosion behavior of 316L stainless steel in high temperature and high pressure water," *Materials at high temperature*, vol. 34(1), pp. 78-86, 2017.
- [10] Y. Wang, H. Sun, N. Li, Y. Xiong, and H. Jing, "Effect of sigma phase precipitation on the pitting corrosion mechanism of duplex stainless steels," *International Journal of Electrochemical Science*, vol. 13, pp. 9868-9887, 2018.
- [11] Y. J. Kim, L. S. Chumbley, and B. Gleeson, "Determination of isothermal transformation diagrams for sigma-phase formation in cast duplex stainless steels CD3MN and CD3MWCuN," *Metallurgical and Materials Transactions A*, vol. 35(11), pp. 3377-3386, 2004.
- [12] G. S. Fonseca, P. M. Oliveira, M. G. Diniz, D. V. Bubnoff, and J. A. Castro, "Sigma phase in super duplex stainless steel: formation, kinetics and microstructural path," *Materials Research*, vol. 20(1), pp. 249-255, 2017.
- [13] I. V. Aguiar, D. P. Escobar, D. B. Santos, and P. J. Modenes, "Microstructure characterization of a duplex stainless steel weld by electron backscattering diffraction and orientation imaging microscopy techniques," *Revista Materia*, vol. 20(1), pp. 212-226, 2015.
- [14] S. N. Li, J. B. Liu, and B. X. Liu, "Phase stability and mechanical properties of sigma phase in Co-Mo system by first principles calculations" *Computational Materials Science*, vol. 98, pp. 424-429, 2015.
- [15] A. Kisasoz, A. Karaaslan, Y. Bayrak, "Effect of etching methods in metallographic studies of duplex stainless steel 2205," *Metal Science and Heat Treatment*, vol. 58, pp. 9-12, 2017.
- [16] K. D. Ramkumar, A. H. Dagur, A. A. Kartha, M. A. Subodh, C. Vishnu, D. Aruna, M. G. V. Kumar, W. S. Abraham, A. Chatterjee, J. Abraham, and J. Abraham, "Microstructure, mechanical properties and biocorrosion behavior of dissimilar welds of AISI 904L and UNS S32750," *Journal of Manufacturing Processes*, vol. 30, pp. 27-40, 2017.
- [17] S. K. Kim, K. Y. Kang, M. S. Kim, and J. M. Lee, "Low-temperature mechanical behavior of super duplex stainless steel with sigma precipitation," *Metals*, vol. 5(3), pp.1732-1745, 2015.
- [18] A. R. Akisanya, U. Obi, and N. C. Renton, "Effect of ageing on phase evolution and mechanical properties of a high tungsten superduplex stainless steel," *Materials Science and Engineering A*, vol. 535, pp. 281-289, 2012.
- [19] D. Zou, Y. Han, W. Zhang, and J. H. Yu, "Sigma phase precipitation and properties of super-duplex stainless steel UNS S32750 aged at the nose temperature," *Journal of Wuhan University of Technology-Mater. Sci. Ed.*, vol. 26(2), pp. 182-185, 2011.
- [20] G. Argandona, J. F. Palacio, C. Berlanga, M. V. Biezma, P. J. Rivero, J. Pena, and R. Rodriguez, "Effect of the temperature in the mechanical properties of austenite, ferrite and sigma phases of duplex stainless steels using hardness, microhardness and nanoindentation techniques. *Metals*, vol. 7(6), pp. 219, 2017.